SUPPLEMENTAL MATERIALS

Characterization of Microfabricated Emitters:

In Pursuit of Improved Nano Electrospray Ionization Performance

Xinyun Wu, Richard D. Oleschuk, Natalie M. Cann*

Department of Chemistry, Queen's University, Kingston, Ontario, Canada K7L 3N6

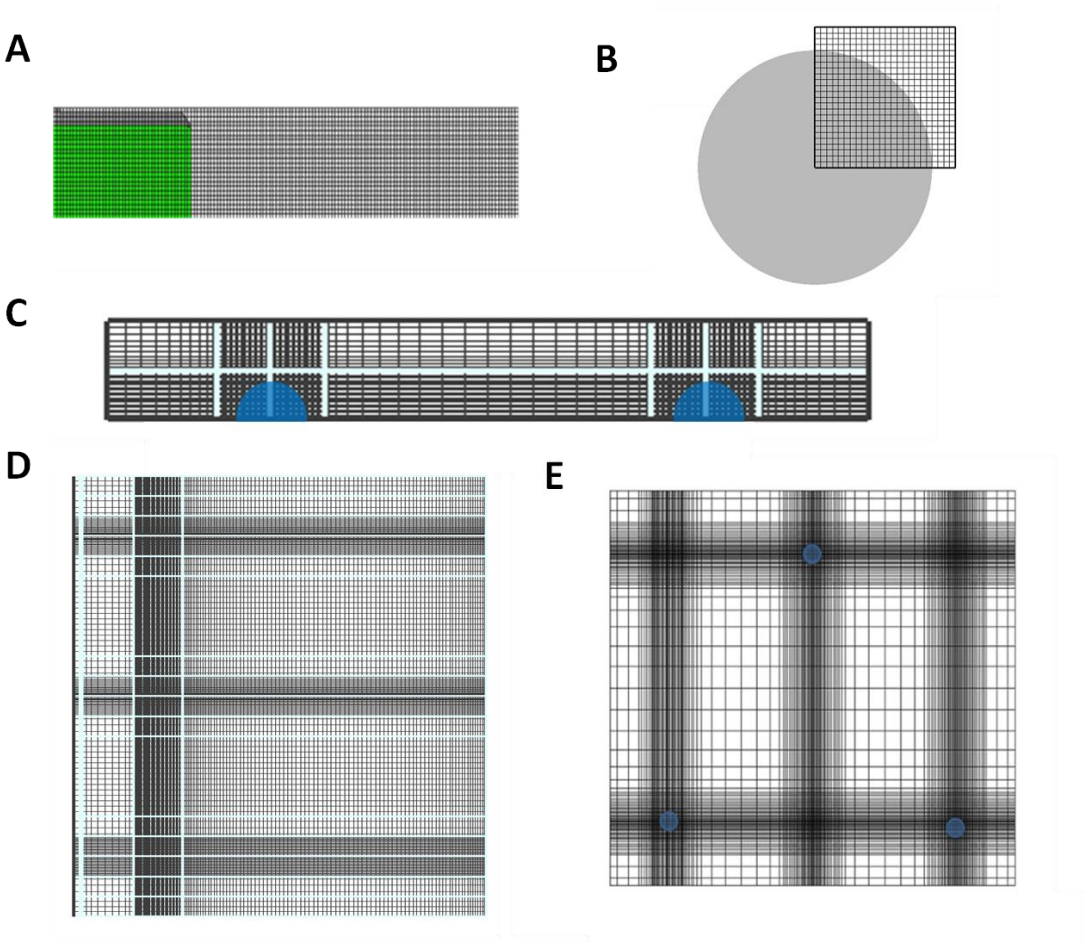

Fig S 1. Mesh applied for different ESI emitter models: (A) X-Z plane of a uniform 2D Cylindrical mesh with 48(120) cells in X(Z) directions; (B) X-Y slice showing the Cartesian mesh for a single-aperture emitter, with 48, 48, and 120 cells in the X, Y, and Z directions respectively; (C) X-Z view showing the non-uniform Cartesian mesh for two-hole emitter model with a total of 180,42,100 cells in the X, Y, and Z directions, respectively; (D) X-Z plane of the non-uniform 3D Cartesian mesh for 3-aligned emitter model with 280, 42, and 100 in the X, Y, and Z directions, respectively; (E) X-Y slice showing the non-uniform Cartesian mesh for the triangular 3-hole emitter model with 160,112, and130 cells in the X ,Y , and Z directions respectively.

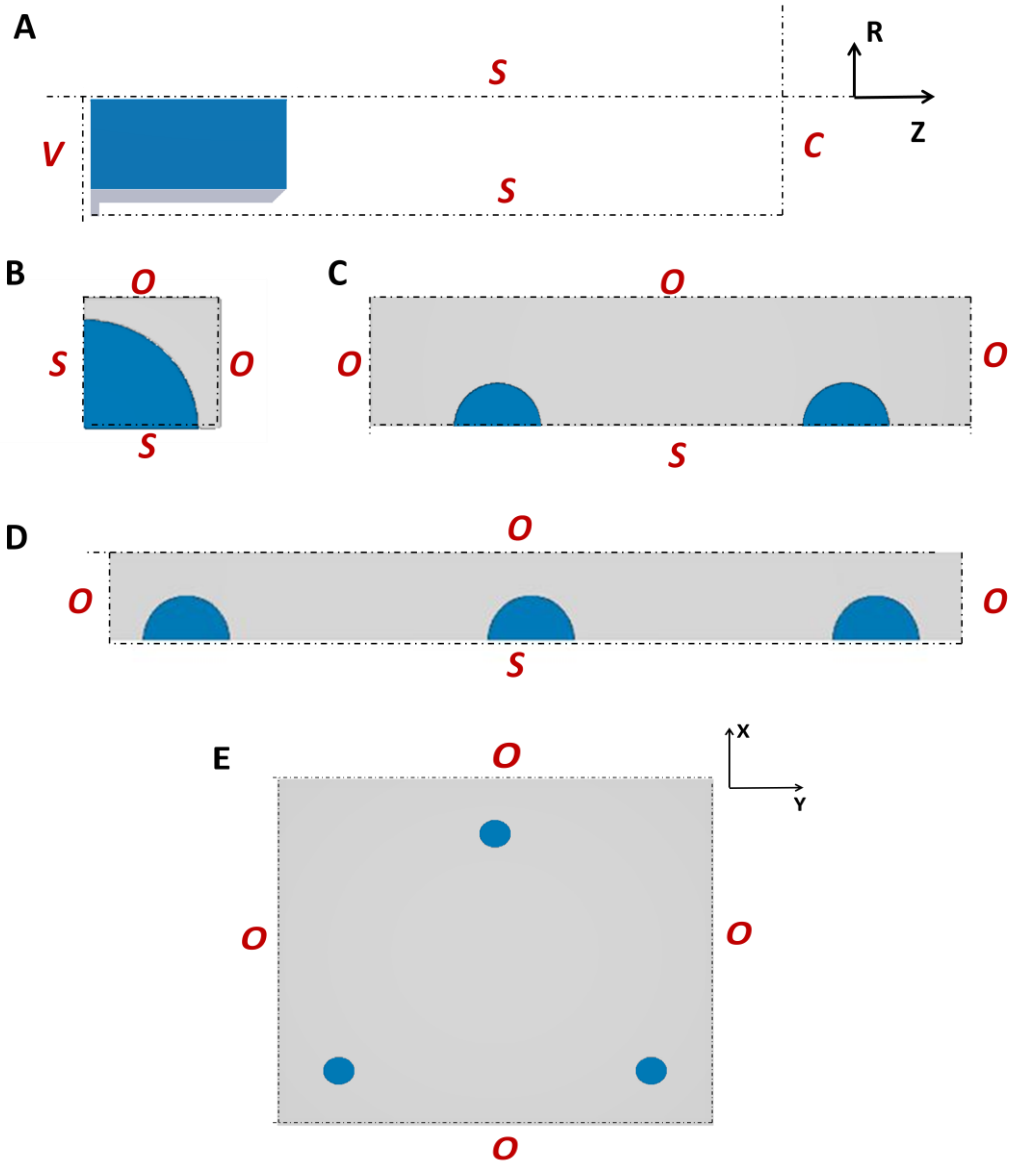

Fig S 2. (A) Boundary conditions for single-aperture emitter model with cylindrical mesh (R-Z plane) (B) Boundary conditions for single aperture emitter model with Cartesian mesh covering one quarter of the computational region (X-Y view); (C) Boundary conditions for two-aperture emitter with Cartesian mesh covering upper half of the model (X-Y view); (D) Boundary conditions for three aligned-aperture emitter with Cartesian mesh covering upper half of the model(X-Y view);(E) Boundary conditions for the triangular three-channel emitter with Cartesian mesh (X-Y view). The capitals indicated in the figure represent the following: V-velocity boundary, S-symmetric boundary, O-outflow boundary, C- continuative boundary. For panels B to E, velocity boundary conditions are applied below and continuative boundary conditions above the images shown.

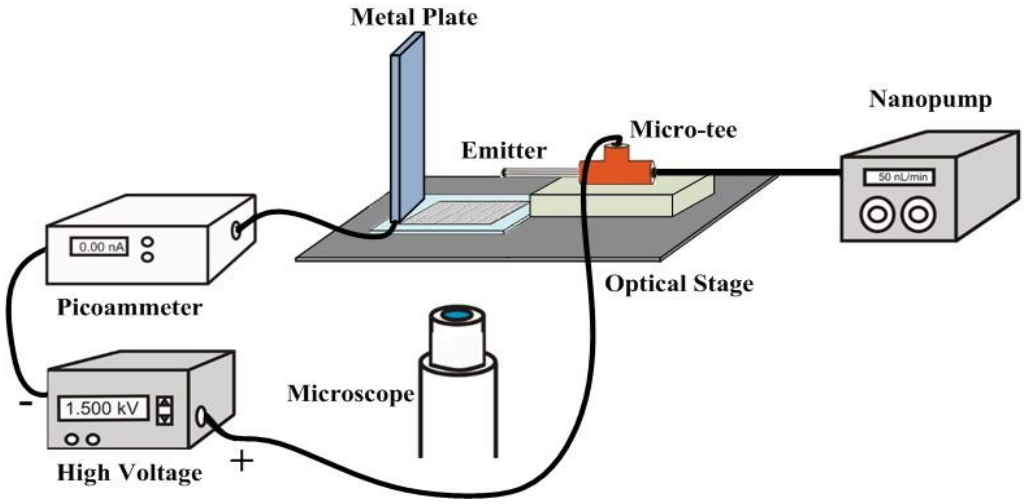

Fig S 3. Schematic of the ESI setup for spray current measurement[4].

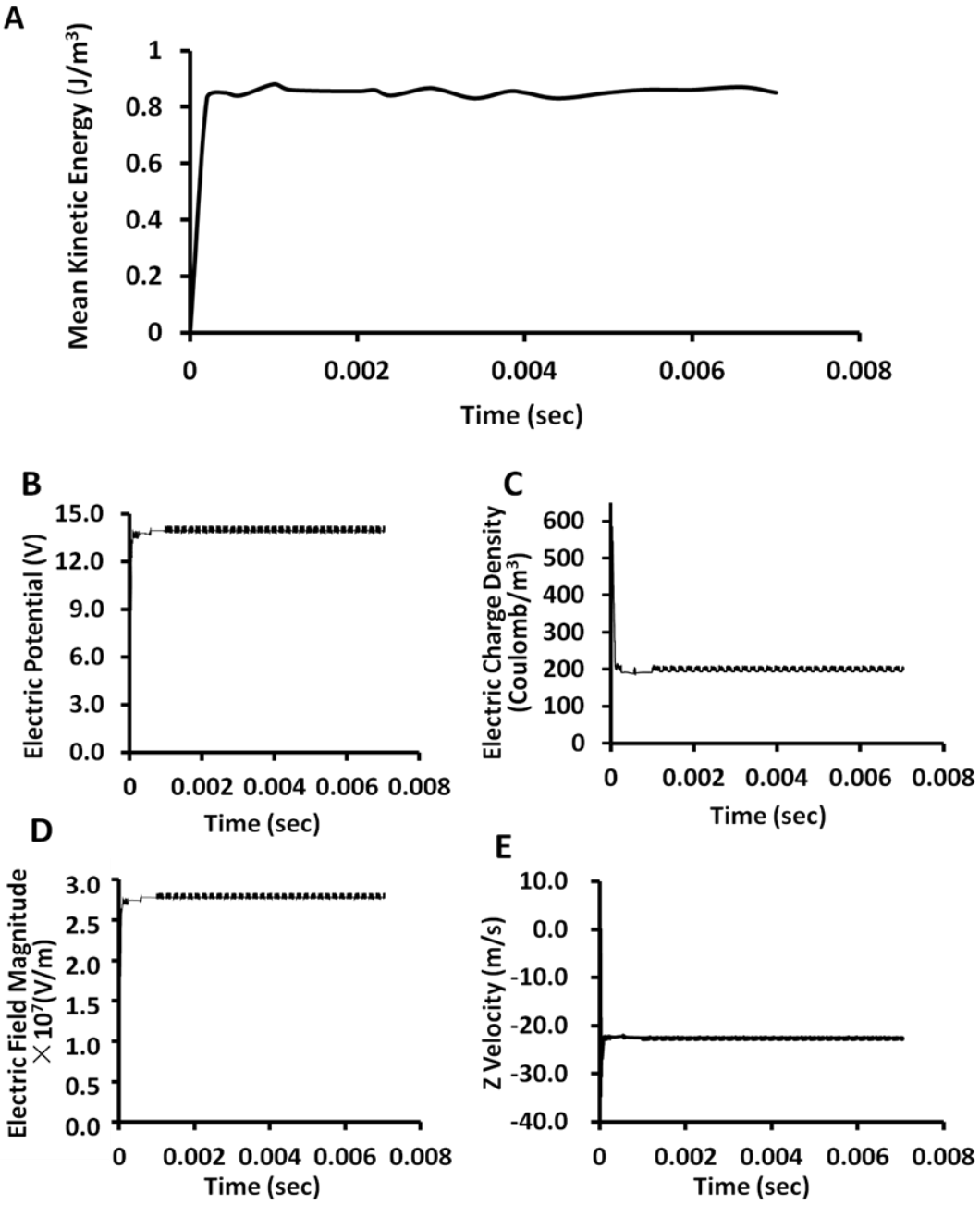

Fig S 4. Quantitative assessment of the steady state for the same system and conditions as in Fig. 2**: (**A) The evolution of mean kinetic energy of the simulation system with time; (B) The evolution of electric potential, electric charge density (C), electric field magnitude (D), and axial velocity (E) probed at a point on the jet surface close to the counter electrode plate.

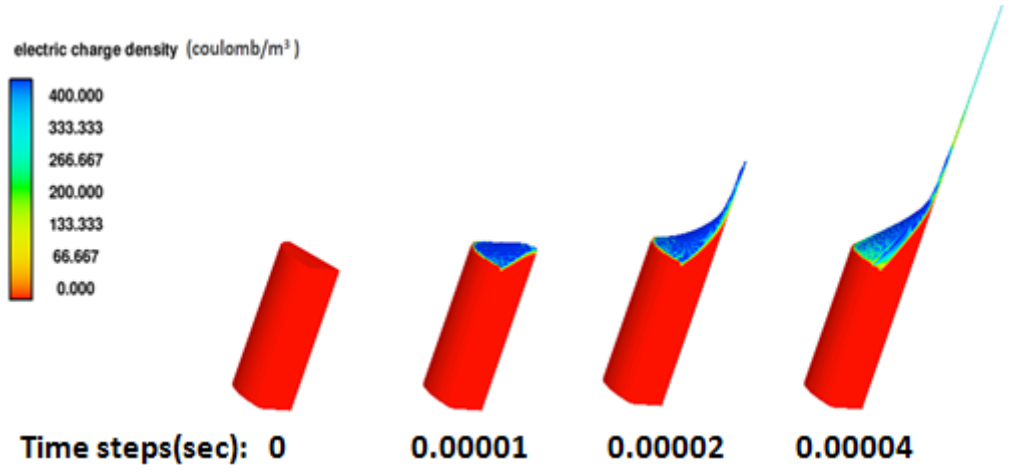

Fig S 5. Generation of the Taylor-cone, for the Cartesian mesh, under an ESI voltage of 800V and inflow velocity 0.09 m/s plotted together with electric charge density contours.

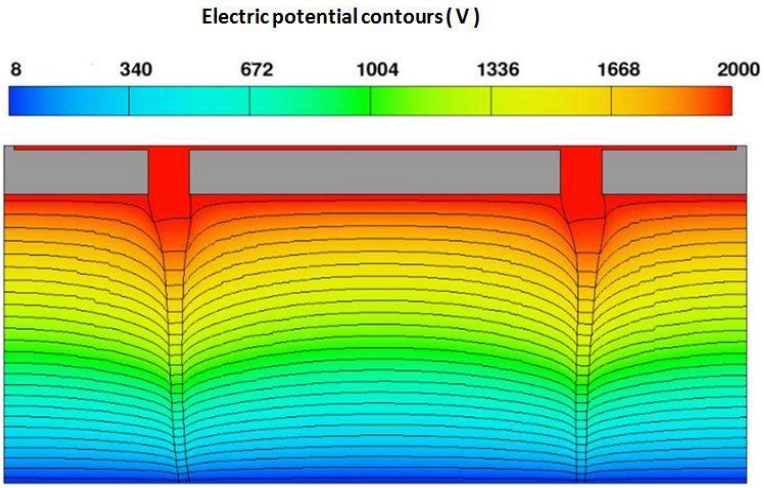

Fig S 6. A snapshot of electrosprays for the two-hole emitter where the channels are well separated, by 180 μm, and demonstrate relatively independent cone-jets. The applied ESI voltage is 2kV and the inflow velocity is 0.09 m/s.